SUPPLEMENTARY INFORMATION

Bipyramidal Gold Nanoparticle-Assisted Plasmonic Photothermal Therapy for Ocular Applications

David Alba-Molina,[*†a,b] Manuel Cano,[*a] Mario Blanco-Blanco,[b] Laura Ortega-Llamas,[b] Yolanda Jiménez-Gómez,[b] Ana Gonzalez-Lopez,[b] Mayelin Perez-Perdomo,[b] Luis Camacho,[a] Juan J. Giner-Casares[†a] and Miguel Gonzalez-Andrades[*b]

[a] Department of Physical Chemistry and Applied Thermodynamics, Chemical Institute for Energy and the Environment (IQUEMA), University of Córdoba, Campus of Rabanales, C3 Marie Curie building, 14071 Córdoba, Spain. E-mail: q82calum@uco.es

[b] Maimonides Biomedical Research Institute of Cordoba (IMIBIC), Department of Ophthalmology, Reina Sofia University Hospital and University of Cordoba, 14004 Cordoba, Spain. E-mail: david.alba@imibic.org; Miguel.gonzalez@gmail.com

[†] These authors contributed equally to this work.

CONTENTS:

1. **Scheme S1.** Summary scheme of the influence of ligand-stabilized on the long-term stability of bipyramidal AuNPs as well as on their PPTT performance.

2. Comparative table of recently reported AuNPs for PPTT with different shapes (**Table S1**).

3. Influence of the thermal treatment on small Au-Seeds (**Fig. S1**).

4. Control of the particle-size of bipyramidal AuNPs during the growth step (**Fig. S2**).

5. Deconvolution of the C 1s peaks of the HR-XPS spectra (**Fig. S3**).

6. Shortening kinetics study of the bipyramidal AuNPs (**Fig. S4** & **Table S2**).

7. Calibration of the NIR laser for PPTT analysis (**Fig. S5 & S6**).

8. Integrity of the bipyramidal AuNPs after NIR laser irradiation (**Fig. S7** & **Table S3**).

9. Experimental procedure for PPTT using the cornea of porcine eyes (**Fig. S8**).

10. Representation of changes in the curved radii and flat radii of the corneal surface (**Fig. S9**).

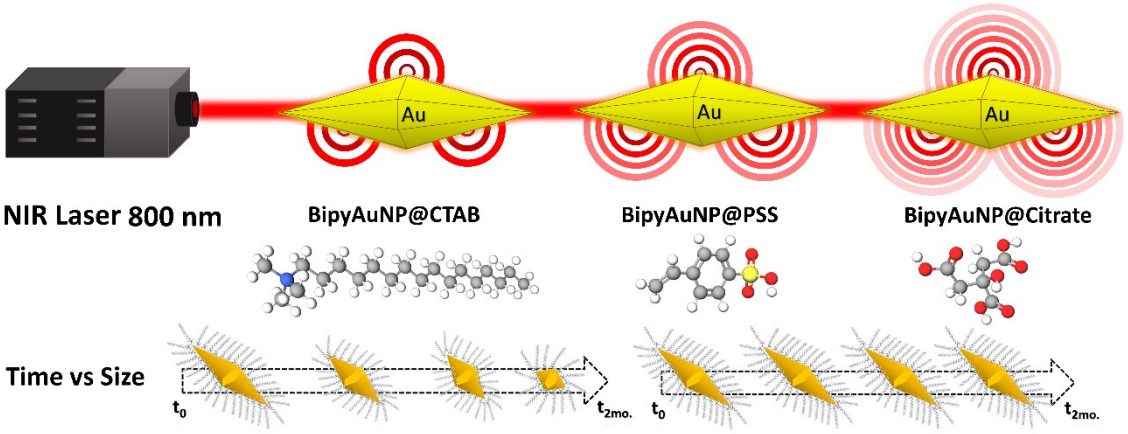

Scheme S1. Summary scheme of the influence of ligand-stabilized on the long-term stability of bipyramidal AuNPs as well as on their PPTT performance.

Comparative table of recently reported AuNPs for PPTT with different shapes:

Table S1. Comparative table of reported AuNPs for PPTT with different shapes.

AuNPs-shape	Stabilizing-ligands	Wavelength NIR laser (nm)	Laser intensity ($W \cdot cm^2$)	Irradiation times (min)	Ref.
Spheres	mPEG-SH	808	0.3	10	[S1]
Rods	CTAB PEG PEG/Lactoferrin	980	0.5	1	[S2]
Shells	PEG	806	1.5	30	[S3]
Cages	Gal@CMaP	808	0.3	30	[S4]
Prisms	PEG	1064	4.5	3	[S5]
Stars	PEG	808	1.0	3	[S6]
Corals	PEG	808	0.5	15	[S7]
Bipyramids	CTAB	808	1.0	10	[S8]
Bipyramids	Citrate	800	2.0	15	This work

Influence of the thermal treatment on small Au-Seeds:

To obtain bipyramidal AuNPs, the seed solution needs to be heated at 80 ºC for 90 minutes to generate twin planes. **Fig. S1** compares the different evolution of the surface plasmon resonance (SPR) band for two different seed solutions, with and without this thermal treatment, respectively. This thermal treatment of small Au-seeds not only increases the Au-seed size but also its uniform crystal structure and long-term stability.

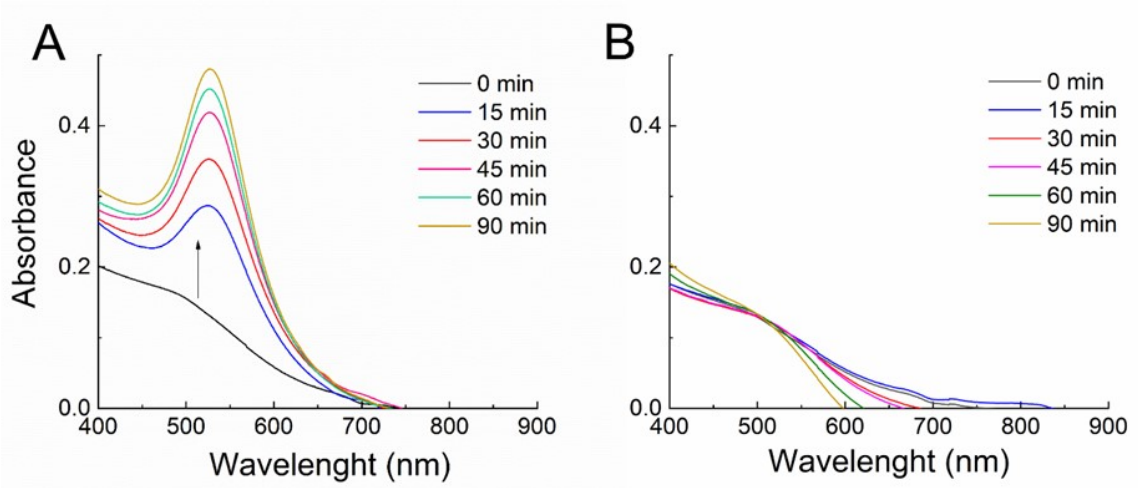

Fig. S1 UV-visible absorption spectra showing the gradual evolution of the SPR band, with (A) and without (B) applied heating at 80 ºC for 90 minutes.

Control of the particle-size of bipyramidal AuNPs during the growth step:

The quantity of the added Au-seeds during the growth step significatively affects to the particle-size of the resulting bipyramidal AuNPs, as it can be observed with the position of their LSPR band (**Fig. S2**). Therefore, the quantity of added Au-seeds allows to effectively control the final size of the bipyramids. In our experiments were added different amounts of seed solutions, ranging from 25 to 600 μL.

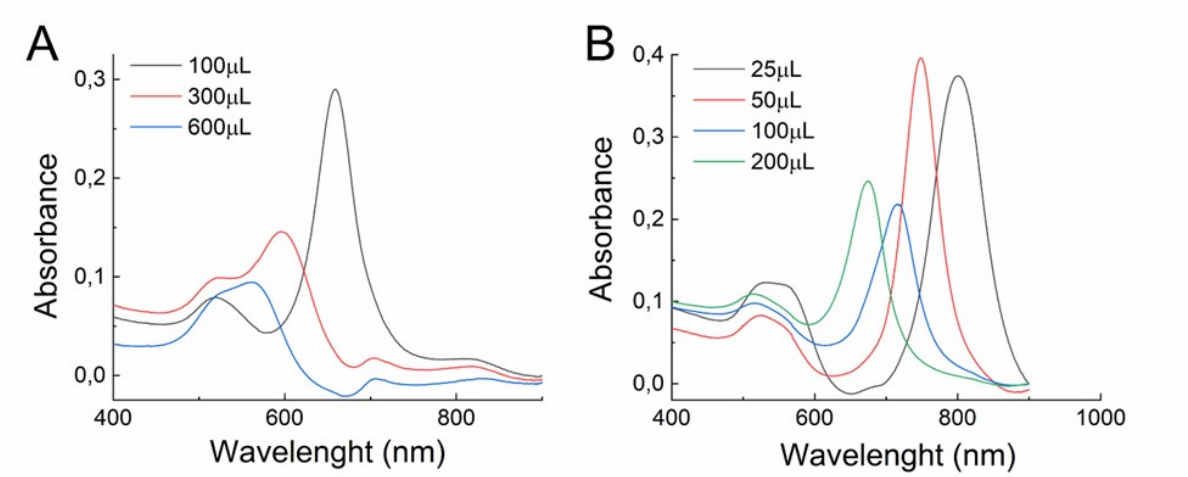

Fig. S2 UV-visible absorption spectra for the resulting bipyramidal AuNPs, which were obtained through the addition of different quantities of Au-seed solution during the growth step. Added volumes of Au seeds ranging from 100 to 600 µL (A), and from 25 to 200 µL (B).

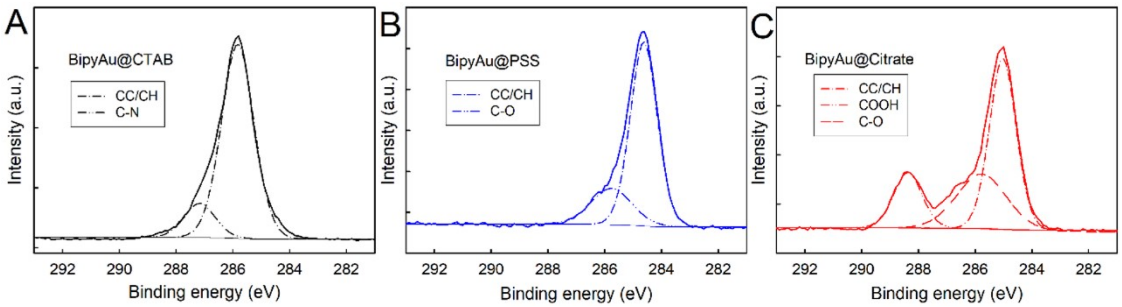

Deconvolution of the C 1s peaks of the HR-XPS spectra:

Fig. S3 Deconvoluted C 1s peaks of HR-XPS spectra of the BipyAu@CTAB (A), BipyAu@PSS (B) and BipyAu@Citrate (C) NPs.

Shortening kinetics study of the bipyramidal AuNPs:

The shortening kinetics study was performed using bipyramidal AuNPs with three different aspect ratio (i.e. obtained by adding different volumes of Au-seed during the growth step) and three different stabilizing-ligands (CTAB, PSS and Citrate). The variation of the LSPR peak of all these 9 samples was measured for two months, without adding accelerators (i.e. O_2 bubbling, high temperatures, or acid concentrations), and keeping a constant temperature of 30 ºC. Fig. S4 summarizes the observed long-term shortening. Overall, similar behavior can be observed independently of the aspect ratio, being stabilizing-ligand the critical parameter. PSS- and Citrate-capped bipyramidal AuNPs provide better stability for 2 months than CTAB-capped ones.

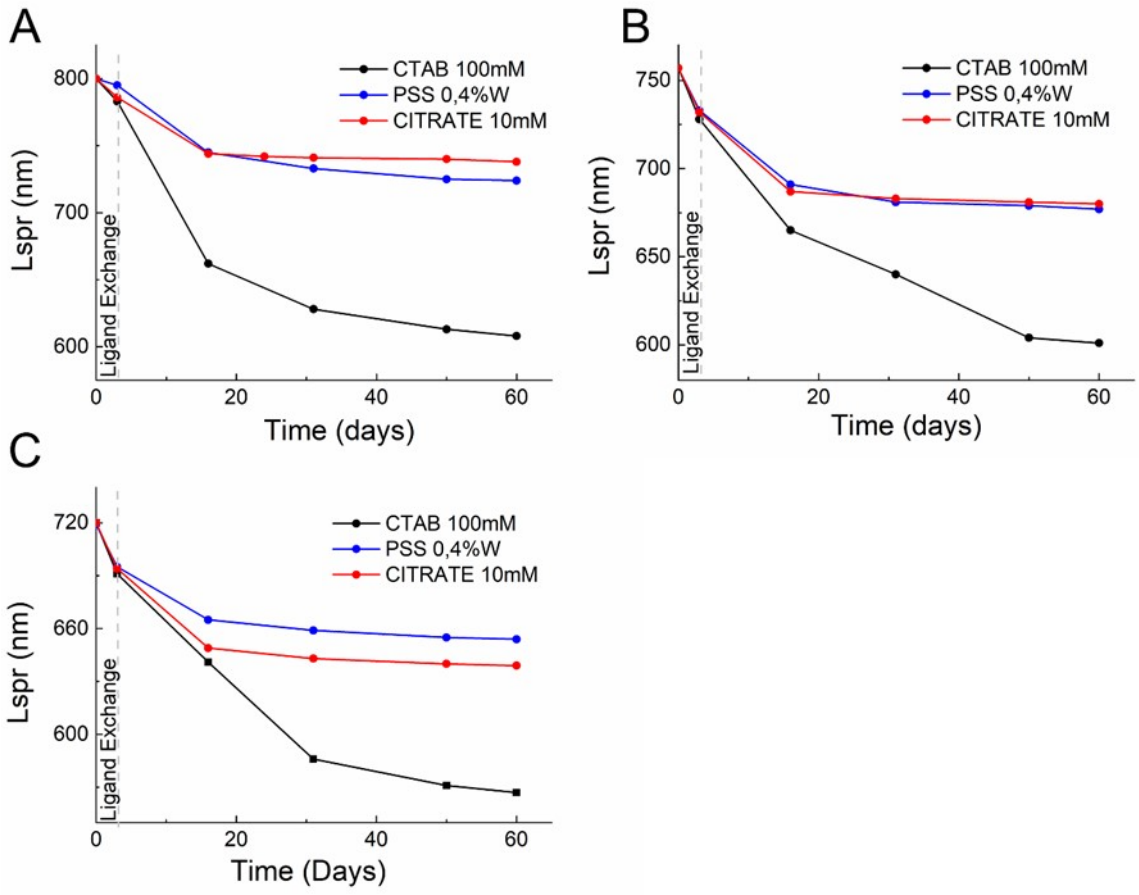

Fig. S4 Monitoring LSPR aging time for two months with different stabilizing-ligand and aspect ratio bipyramidal AuNPs. (A) LSPR aging for the larger bipyramidal AuNPs obtained with 25 µL of Au-seed solution during growth step, (B) LSPR aging for bipyramidal AuNPs with intermediate size (50 µL of Au seed solution added) and (C) LSPR aging the shorter bipyramidal AuNPs (adding 100 µL of Au-seed solution).

Table S2. Values of λ_0, λ_i and k employed for fitting with eq (1).

	λ_0 (nm)	λ_i (nm)	K
BipyAu@CTAB	869.48	751.74	0.239
BipyAu@PSS	871.88	792.70	0.309
BipyAu@Citrate	868.43	784.46	0.254

Calibration of the NIR laser for PPTT analysis:

The heating rate and temperature increment were calibrated by NIR laser irradiation at a wavelength of 808 ± 5 nm (see used assembly in **Fig. S5**) and using different laser intensities (from 0.5 to 2.0 $W \cdot cm^{-2}$) for 15 minutes of exposition time. For this, we first measured the heating rate of an empty cuvette, containing only pure water and with PBS solution (1X, pH 7.4) (**Fig. S6**). The heating rate measured with the PBS solution was employed as control, which was subtracted to those obtained with samples containing bipyramidal AuNPs.

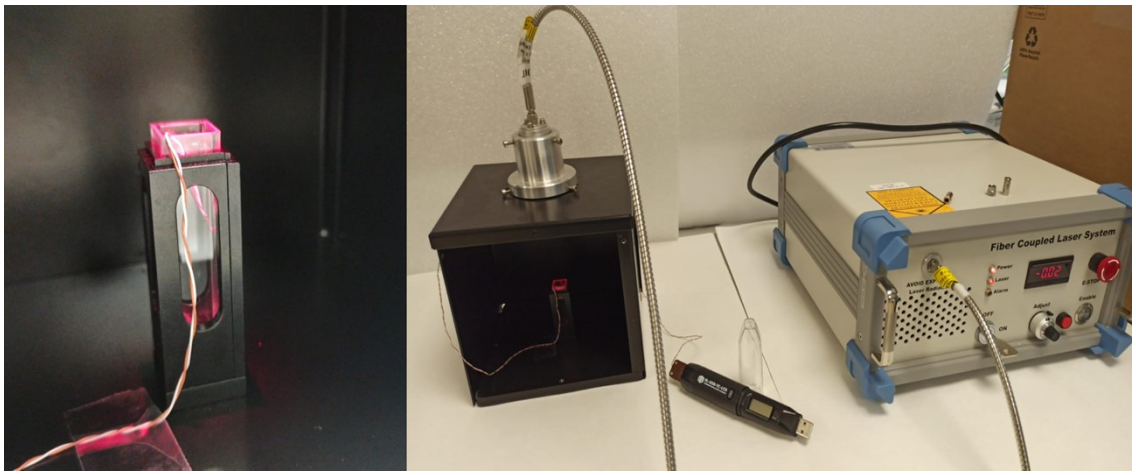

Fig. S5 Pictures of the assembly used for the photothermal analysis with the bipyramidal AuNPs.

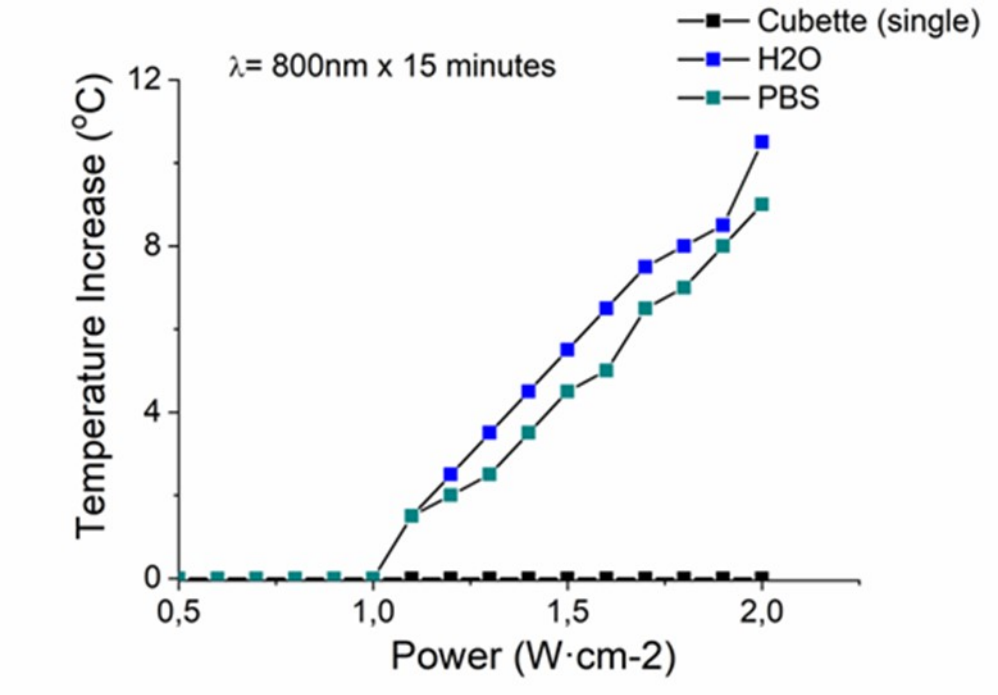

Fig. S6 Typical calibration of the NIR laser irradiation at 808 nm for 15 min. Graphical representation of the resulting temperature increase against different laser intensities for three control samples: Empty cuvette, ultrapure water and PBS (1X, pH 7.4).

Integrity of the bipyramidal AuNPs after NIR laser irradiation:

The integrity of the different bipyramidal AuNPs was investigated by measuring their LSPR bands (Table S2) and TEM images (Fig. S7), after NIR laser irradiation at 808 nm for 15 minutes. Fig. S7 confirms that, after NIR irradiation, the bipyramidal AuNPs retained their shape and size. Table S3 showed that BipyAu@Citrate suffers greater displacement of LSPR band than BipyAu@CTAB and BipyAu@PSS NPs, as expected due to the higher temperature increase.

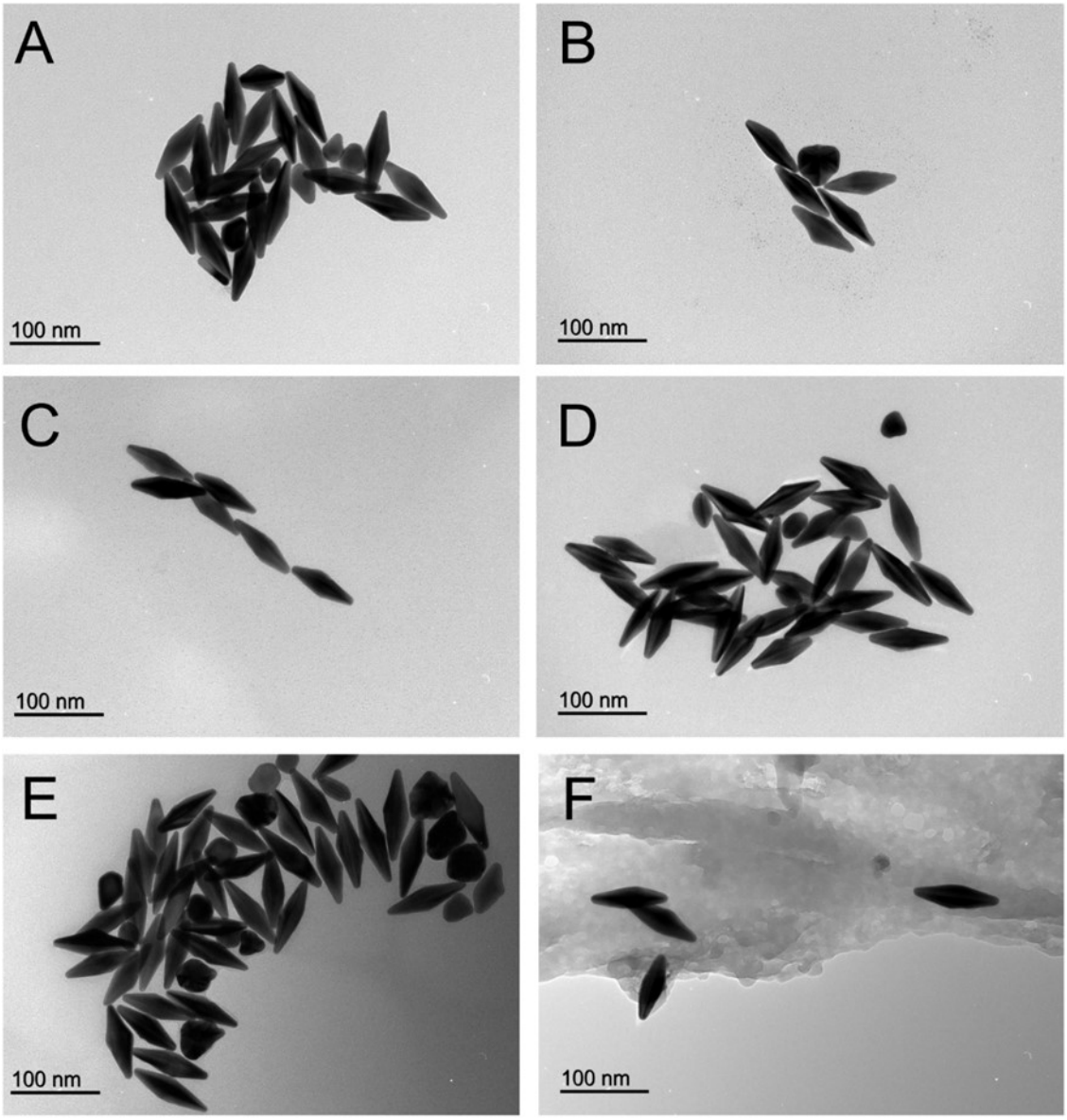

Fig. S7 Representative TEM images of bipyramidal AuNPs with different stabilizing-ligands, before (A,C,E) and after (B,D,F) NIR laser irradiation: (A,B) BipyAu@CTAB, (C,D) BipyAu@PSS, and (E,F) BipyAu@Citrate NPs, respectively.

Table S3. Representative summary table with the resulting LSPR band values, before and after NIR laser irradiation, obtained with the bipyramidal AuNPs shown in **Fig. S7**.

	LSPR peak before NIR (nm)	**LSPR peak after NIR (nm)**
BipyAu@CTAB	785	782
BipyAu@PSS	798	798
BipyAu@Citrate	795	786

Experimental procedure for PPTT using the cornea of porcine eyes:

Porcine eyes were evaluated for PPTT treatment. For this ex vivo study, the corneal epithelium was removed mechanically using a surgical blade to facilitate AuNPs internalization. Then, a volume of 600 µL of BipyAu@Citrate NPs with [Au^0]: 15.2 mM (0.18 µg Au) was applied to the cornea surface with caution to keep the AuNPs dispersion concentrated into the central area of the cornea. Similarly, and for the control porcine eyes, a volume of 600 µL of the PBS solution (1X, pH 7.4) was applied. Subsequently, both porcine eyes groups were irradiated with NIR laser of 808 ± 5 nm at 1 $W \cdot cm^{-2}$ for 15 minutes. Then, eyes were rinsed with 1 mL of PBS (1X, pH 7.4) to remove the BipyAu@Citrate NPs. **Fig. S8** shows representative photographs of the cornea of porcine eyes, where a clear flattening corneal surface after PPTT treatment can be observed.

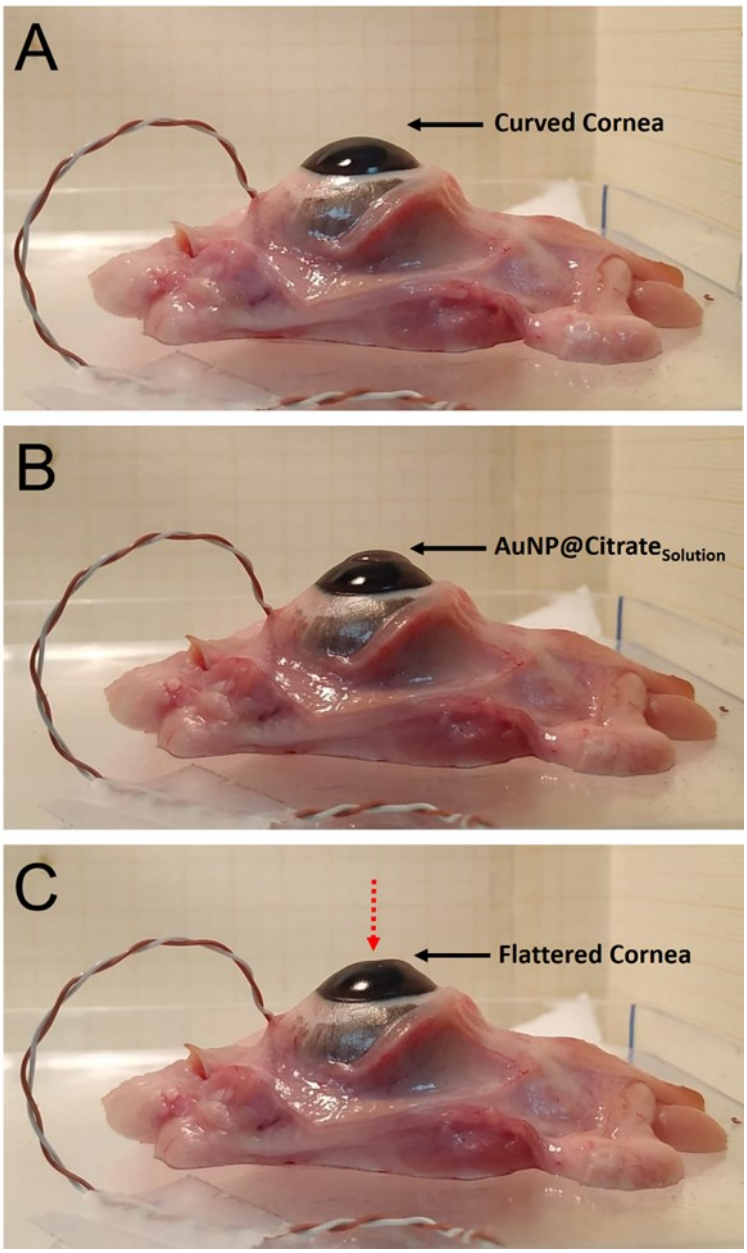

Fig. S8 Representative photographs of porcine corneas, before and after PPTT treatment using BipyAu@Citrate NPs: (A) Curved porcine cornea without epithelium and before PPTT treatment; (B) Curved porcine cornea without epithelium and after the addition of BipyAu@Citrate NPs dispersion, but PPTT treatment; (C) Flattened porcine cornea resulting after PPTT treatment and rinsed with PBS.

Representation of changes in the curved radii and flat radii of the corneal surface:

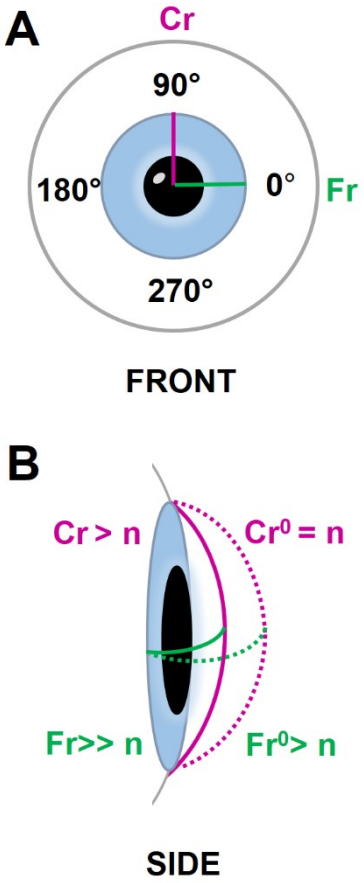

Fig. S9 Schematic representation of the changes in the curved and flat radii of the corneal surface. (A) Front view of the corneal surface showing the flat radii (Fr, in green) along 0-180º axis and the curved radii (Cr, in pink) along the 90-270º axis. (B) Side view of the corneal surface, illustrating the changes before and after treatment with BipyAu@Citrate NPs + NIR. Initially, the radii are represented as n (Cr^{o} = n, Fr^{o} > n). After treatment, Cr > n and Fr >> n.

References:

S1 W. Yang, B. Xia, L. Wang, S. Ma, H. Liang, *Mater. Today Sustain.*, 2021, **13**, 100078.

S2 H. Yang, H. He, Z. Tong, H. Xia, Z. Mao, C. Gao, *J. Colloid Interf. Sci.*, 2020, **565**, 186-196.

S3 Y. He, K. Laugesen, D. Kamp, S. A. Sultan, L. B. Oddershede, L. Jauffred, *Cancer Nanotechnol.,* 2019, **10**, 8.

S4 S. Wang, Y. Song, K. Cao, L. Zhang, X. Fang, F. Chen, S. Feng, F. Yan, *Acta Biomaterialia*, 2021, **134**, 621-632.

S5 M. Moros, A. Lewinska, F. Merola, P. Ferraro, M. Wnuk, A. Tino, C. Tortiglione, *ACS Appl. Mater. Interfaces*, 2020, **12**, 13718-13730.

S6 S. Zhu, S. Xu, Y. Guo, H. Zhang, K. Ma, J. Wang, Q. Zhao, L. Zhou, W. Cai, *ACS Nano,* 2023, **17**, 10300-10312.

S7 Y. Xing, T. Kang, X. Luo, J. Zhu, P. Wu, C. Cai, *J. Mater. Chem. B*, 2019, **7**, 6224-6231.

S8 X. Wu, L. Mu, M. Chen, S. Liang, Y. Wang, G. She, W. Shi, *ACS Appl. Bio Mater.,* 2019, **2**, 2668-2675.